Eur. Phys. J. B **23**, 69–77 (2001)

THE EUROPEAN PHYSICAL JOURNAL B

EDP Sciences
© Società Italiana di Fisica
Springer-Verlag 2001

Strong impact of the electron-photon matrix element on angle-resolved photoelectron spectra of $Sr_2CuO_2Cl_2$

S. Haffner, M. Schmidt, P.J. Benning, C.G. Olson, L.L. Miller, and D.W. Lynch

Department of Physics and Astronomy and Ames Laboratory, US Department of Energy, Iowa State University, Ames, Iowa 50011, USA

Received 10 January 2000 and Received in final form 15 January 2001

Abstract. In recent years insight has been gained into the electronic structure of layered cuprates using angle-resolved photoelectron spectroscopy. In many of these studies it is assumed that the electron-photon matrix element follows the trends set by the atomic photoionization cross sections and does not influence lineshape, dispersion and the **k**-dependence of the spectral intensity. In this study using $Sr_2CuO_2Cl_2$ as an example it will be shown that the electron-photon matrix element can have a strong impact on both strength and shape of a feature in an angle-resolved photoelectron spectrum of a layered cuprate which can strongly affect information on character and the momentum-dependence of the energy and spectral weight of a state deduced from the spectra. The results of this study put an emphasis on the need to employ the whole parameter range of the ARPES method to get reliable information on the spectral function of cuprates for which purpose synchrotron radiation is an uniquely suited tool.

PACS. 74.72.Jt Other cuprates – 79.60.-i Photoemission and photoelectron spectra – 74.25.Jb Electronic structure

1 Introduction

Recently angle-resolved photoelectron spectroscopy (ARPES) has played an important role in the study of layered cuprate compounds as, for example, the high-temperature superconductors. Results obtained by ARPES are, for example, the existence of a Fermi surface in the normal state compatible with the Luttinger theorem [1–3] and the observation of the superconducting gap and its anisotropy, as well as a gap in the normal state in the underdoped regime [4–8]. One of the appealing features of ARPES is that the spectral intensity of an electron distribution curve (EDC) is directly proportional to the electron-photon matrix element weighted spectral function [9]. Direct insight into the character, symmetry, dispersion and lineshape of the single-electron excitations can therefore be gained which currently is not possible with any other experimental method. ARPES also allows a direct comparison to theoretical models, as the spectral function is directly proportional to the imaginary part of the one-electron Greens function of many-body theory [10].

Nonetheless, one has to stress that the spectral intensity observed in an EDC is proportional to the electron-photon matrix element weighted spectral function and not the spectral function itself. In many ARPES studies of layered cuprates it is assumed that the matrix element follows the trends given by the atomic photoionization cross sections although calculations suggest that the relationship between ARPES intensities and the underlying electronic structure can be quite complicated for a layered cuprate [11]. In the following, using angle-resolved photoelectron spectra of $Sr_2CuO_2Cl_2$ as an example, it will be experimentally demonstrated that for layered cuprates the electron-photon matrix element can have a significant impact on the relative spectral intensity *and* the shape of a feature in an ARPES spectrum which can strongly affect the information on character and the momentum dependence of energy and spectral weight of a band deduced from the ARPES spectra.

The paper is organized as follows: Firstly, information on $Sr_2CuO_2Cl_2$ relevant for an understanding of this study is given. Then our experimental procedures will be described. The remainder of the paper is devoted to a discussion of the impact of the electron-photon matrix element on information on the electronic structure of layered cuprates which can be gathered using ARPES: the character of a state using the dependence of the photoemission-intensity related to the particular state under consideration on photon energy, the **k**-dependence of the spectral weight and the lineshape and dispersion of an excitation.

2 Why $Sr_2CuO_2Cl_2$?

$Sr_2CuO_2Cl_2$ was chosen as it can be regarded as a model system for the physics of layered cuprates having CuO_2 planes as their fundamental building block. $Sr_2CuO_2Cl_2$

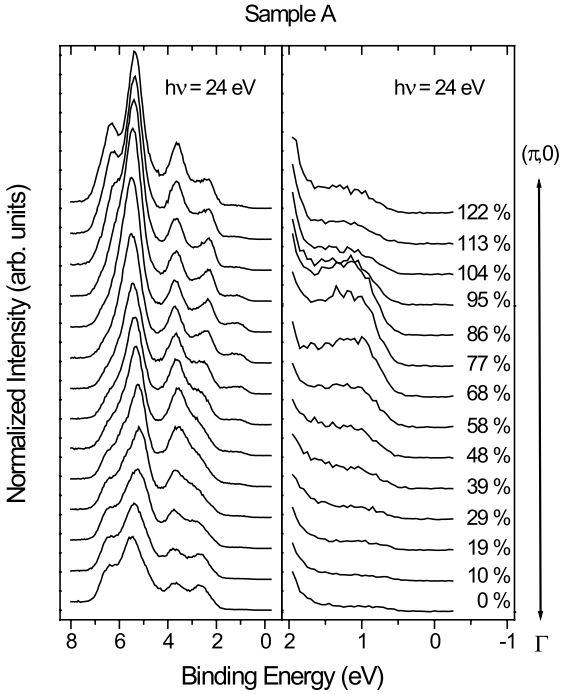

Fig. 1. ARPES VB spectra of $Sr_2CuO_2Cl_2$ recorded along the Γ to (π,0) direction in **k**-space using 24 eV photon energy. Left panel: full VB. Right panel: expanded-scale plot of the lowest-lying states.

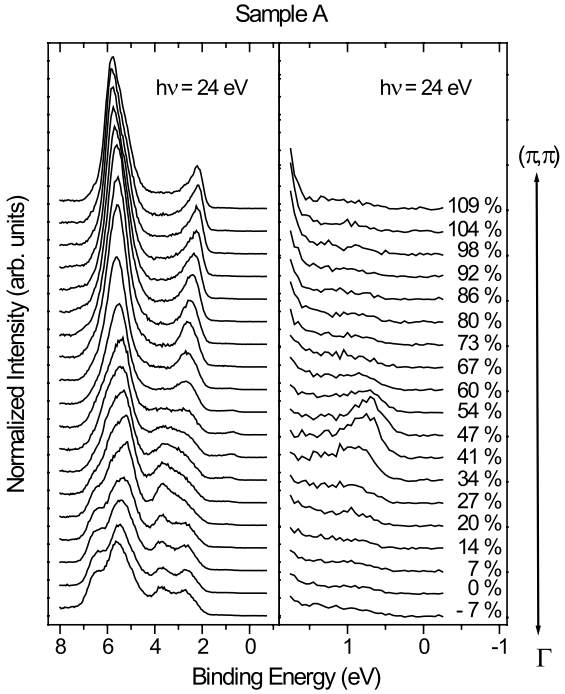

Fig. 2. ARPES VB spectra of $Sr_2CuO_2Cl_2$ recorded along the Γ to (π,π) direction in **k**-space using 24 eV photon energy. Left panel: full VB. Right panel: expanded-scale plot of the lowest-lying states.

is closely related to the undoped parent compounds of the high-temperature superconductors as it is also an antiferromagnetic insulator having a Néel temperature of 255 K [12]. The CuO_2 planes in $Sr_2CuO_2Cl_2$ are undoped (half-filling); therefore the spectral intensity in an EDC related to the CuO_2 plane gives information about the dynamics of a single hole (the hole created by photoionization) in a CuO_2 plane. The ARPES experiments in this study were performed at 300 K. Although there is no long-range antiferromagnetic order at room temperature in $Sr_2CuO_2Cl_2$, the antiferromagnetic correlation length is still two orders of magnitude larger than the Cu-O distance [12]. Therefore photoemission, as a fast and local probe, still sees the effect of antiferromagnetic order even 50 K above the Néel temperature [13].

The dynamics of a hole in a two-dimensional antiferromagnetic background is of fundamental interest itself and there have been numerous theoretical [14] and experimental [13,15–18] studies of this subject. Of primary interest are the lowest lying states split-off from the main VB, the so-called first electron-removal states, which, according to most theoretical results, should be comprised of a low binding energy quasiparticle peak ascribed to the so-called Zhang-Rice singlet [19] (ZRS) followed by incoherent spectral weight at higher binding energy due to quasiparticle dressing [14]. The first electron-removal states of $Sr_2CuO_2Cl_2$ indeed show a well-developed low binding energy peak followed by additional spectral weight at higher binding energies for **k**-vectors along the Γ to (π,π) direction of the first Brillouin zone (BZ) of the CuO_2 plane [20]. In contrast to most other layered cuprates, ARPES spectra of $Sr_2CuO_2Cl_2$ also show a very structured main VB (see Figs. 1 and 2) and even an assignment of features of the main VB spectra to individual bands is possible [21,22]. In this work we will not further elaborate on the physics behind the VB electronic structure of $Sr_2CuO_2Cl_2$ but rather use both the lowest-lying, as well as the main VB states, for a study of the impact of the electron-photon matrix element on ARPES spectra of layered cuprates. The VB states of $Sr_2CuO_2Cl_2$ are well-suited for this purpose since there are no complications due to apical oxygen atoms as in $La_{2-x}Sr_xCuO_4$, no states derived from Cu-O chains as in $YBa_2Cu_3O_x$, no superstructure effects as in $Bi_2Sr_2CaCu_2O_8$ (BSCCO) and, finally, no Fermi energy cut-offs given the insulating nature of this material.

3 Experimental

The angle-resolved photoelectron spectra were recorded in the EDC or constant-initial-state (CIS) modes of photoelectron spectroscopy on the storage ring, Aladdin, at the University of Wisconsin-Madison Synchrotron Radiation Center, on the Ames Laboratory/Montana State University ERG/SEYA beamline. A 50 mm radius hemispherical analyzer having a 2° full angular acceptance angle was used which corresponds to a **k**-resolution of 0.06 $Å^{-1}$ and 0.16 $Å^{-1}$ (5% and 14% of the distance between Γ and (π,π)) for states of 1 eV binding energy and 20 and 90 eV photon energy, respectively. EDC spectra of the full VB

and CIS spectra were recorded using 15 eV pass energy while for the first electron-removal states 10 eV pass energy was used. The total energy resolution was 102 and 115 meV for 20 and 35 eV photons, respectively, for 10 eV pass energy. For 15 eV pass energy the total energy resolution was 151 and 340 meV for 20 and 90 eV photon energy, respectively. The angle of incidence of the photons was $\sim$40° with respect to the sample surface normal with the electric field vector being polarized in a horizontal plane. The $Sr_2CuO_2Cl_2$ single crystals were grown as described elsewhere [23]. The samples were oriented *ex situ* by Laue-backscattering and mounted with the Cu-O oxygen bonds in a horizontal/vertical plane. The samples were cleaved (cleavage plane parallel to CuO_2 planes) in the experimental chamber in a vacuum better than 6×10^{-11} torr and the sample alignment was confirmed *in situ* by using the symmetry of the dispersion of spectral features at high-symmetry points. All EDC and CIS spectra were recorded at room temperature and were normalized to the photon flux. The Fermi edge of a platinum foil in electrical contact with the sample was used as binding energy reference. EDC's recorded at a given **k**-vector and photon energy showed no dependence of the binding energy and lineshape on photon flux for an individual sample. We observed overall shifts of the binding energy scale of $\sim$0.1 eV between different samples. This may be due to changed charging conditions for different samples but can be also another manifestation of matrix element effects as the angle of the sample surface normals with a horizontal plane varied from +10° to −10° for different samples which can have an influence on the spectra *via* the electron-photon matrix element. Nonetheless, we want to stress that the effects discussed in the following were reproducibly observed (besides the aforementioned overall energy shift) on four samples and that in our discussion we will only directly compare spectra which were recorded using the same sample and sample cleave.

4 Results and discussion

Before we describe our results in detail, we want to convince the reader that our $Sr_2CuO_2Cl_2$ ARPES spectra were not recorded using extraordinary samples, or sample cleaves, and that they are consistent with all previous ARPES data on $Sr_2CuO_2Cl_2$ or the closely related $Ca_2CuO_2Cl_2$ [13,15–17,21,22]. Figures 1 and 2 show full VB spectra of $Sr_2CuO_2Cl_2$ (sample A, sample surface normal +10° off a horizontal plane) for 24 eV photon energy along the Γ to (π,0) and Γ to (π,π) directions in **k**-space, respectively. Note the split-off first electron-removal states and the main VB between 2 and 7 eV. Comparing to previous results, which were recorded using different photon energies and/or emission plane-polarization plane geometries than used in recording the data presented in Figures 1 and 2, we notice that there is qualitative agreement both for the first electron-removal states as well as for the main VB: for **k**-vectors from Γ to (π,π), for example, we observe a distinct low energy peak for the first electron-removal states which has its lowest binding energy at $\sim$(π/2,π/2) and the majority of its spectral intensity for **k**-vectors before (π/2,π/2) as reported in the literature. Along Γ to (π,0) we also observe the first electron-removal states to have the form of a broad peak which can only be observed in a range of **k**-vectors from $\sim$50% to $\sim$85% of the distance between Γ and (π,0) and which has its maximum spectral intensity at $\sim$70% of the distance between Γ and (π,0). And in the main VB, peaks due to the non-bonding O 2p states reported in references [21,22] at Γ, (π,0) and (π,π) can be easily identified at $\sim$2.75/3.75, $\sim$3.7 and $\sim$2.2 eV, respectively. Nonetheless, in the following we will show that despite the good overall agreement between data sets recorded using different photon energies and/or emission plane-polarization plane geometries they differ in such important aspects as, for example, spectral intensity as a function of **k** and lineshape of a feature due to the electron-photon matrix element.

4.1 Photon energy dependence of the intensity of main VB features of $Sr_2CuO_2Cl_2$

In photoelectron spectroscopy information about the character of a state can be gained by studying the intensity of emission from that state as a function of photon energy. If, for example, the photoemission intensity from a state as a function of photon energy qualitatively resembles that of the atomic Cu 3d photoionization cross section, one would assert that this state is derived from Cu 3d orbitals. In a solid the final state reached upon photoexcitation can be quite different from a free electron parabola, especially for small excitation energies. It is therefore not unexpected if the photoemission intensity from a certain initial state of a solid fails to follow the trends set by the atomic photoionization cross section of the contributing orbitals. For BSCCO and $YBa_2Cu_3O_{6.9}$ it was previously noticed that for some photon energies the photon energy dependence of the emission at the Fermi level cannot be described by a superposition of the O 2p and Cu 3d atomic photoionization cross sections [24] although no resonant channel is involved.

In order to achieve a reasonable **k**-resolution, ARPES experiments on layered cuprates are generally performed using photon energies from 15 up to 80 eV. Typically it is assumed that for these relatively high energies the final state reached upon photoexcitation is a continuum with minimal structure. It is expected then that atomic photoionization cross sections should be capable of describing the variation of the intensity of a spectral feature at least in a qualitative manner. To test this assumption we looked at the photon energy dependence of the spectral intensity of some well understood features in the main VB of $Sr_2CuO_2Cl_2$ at normal emission.

Figure 3 shows VB ARPES spectra of $Sr_2CuO_2Cl_2$ (sample A) recorded at normal emission for 20, 22 and 24 eV photon energy. Figure 4 presents VB ARPES spectra (sample A) recorded at normal emission from 40 to 80 eV photon energy. In the main VB four spectral features can be observed for all photon energies (labeled A, B, E and F) at $\sim$2.65, $\sim$3.7, $\sim$5.4 and $\sim$6.15 eV. For 20 eV

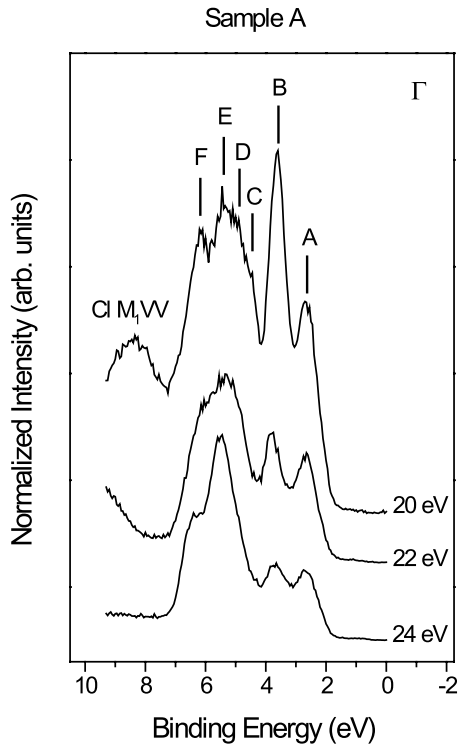

Fig. 3. VB ARPES spectra of $Sr_2CuO_2Cl_2$ recorded at normal emission for 20 to 24 eV photon energy. Features in the main VB are denoted by letters A to F. For 20 eV photon energy a peak due to the Cl M_1VV Auger is observed at ∼8.2 eV binding energy.

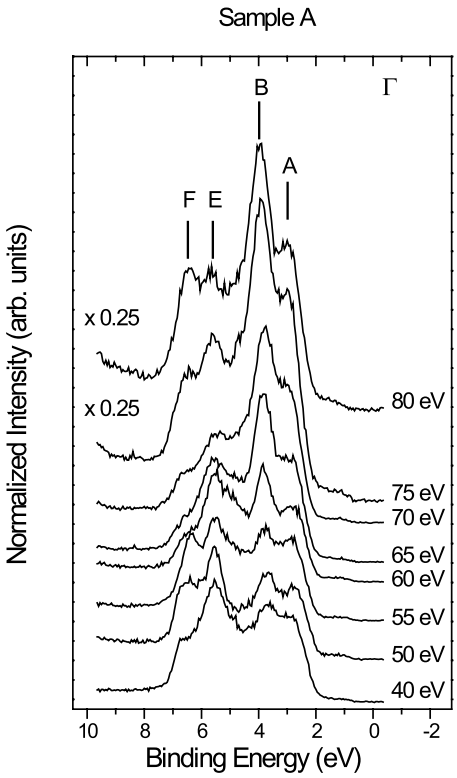

Fig. 4. VB ARPES spectra of $Sr_2CuO_2Cl_2$ recorded at normal emission for 40 to 80 eV photon energy. Features in the main VB are denoted using the same notation as in Figure 3. Note that the 75 and 80 eV spectra are on a different y-scale.

photon energy two more features are visible which comprise shoulders (labeled C and D) at the low binding energy side of peak E at ∼4.5 and ∼4.85 eV. There are small changes in the positions of the peaks with photon energy (∼0.2 eV for photon energies from 20 to 80 eV). It has been already demonstrated in reference [22] that the main VB features in the ARPES spectra of $Sr_2CuO_2Cl_2$ can be successfully assigned to individual bands if correlation effects are appropriately accounted for in the band structure calculation. At Γ and for the emission plane-polarization plane geometry used in our experiment, for example, the calculation predicts features in the main VB of $Sr_2CuO_2Cl_2$ at 2.69, 3.69, 4.58, 4.92, 5.57 and 5.88 eV which are in good agreement with the positions of features A to F in Figure 3. According to reference [22] peak A is then due to a state which is nearly completely derived from in-plane O $2p$ orbitals while feature B is an out-of-plane state due to O $2p_z$ (57%) and Cl $3p_z$ (43%) orbitals. Feature C is derived mostly from Cu $3d_{3z^2-r^2}$ (64%) and Cl $3p_z$ (33%) orbitals, feature D is dominated by in-plane Cu $3d$ orbitals while peak E is due to another nearly "pure" O $2p$ state. Finally, feature F can be assigned to a state predominantly derived from out-of-plane Cu $3d$ (Cu $3d$ 80%, Cl $3p$ 20%) orbitals.

Let us look now at the photon-energy dependence of the spectral intensity of features A to F. In the range from 20 to 24 eV photon energy, all features except peak E lose intensity on going from 20 to 24 eV, with the effect especially marked for peaks B, C and D. The ratio of the atomic Cl $3p$, O $2p$ and Cu $3d$ photoionization cross sections is 2 : 1 : 0.7 at 20 and 0.5 : 1 : 0.8 at 25 eV with a strong decrease of the Cl $3p$ and a slight decrease/increase of the O $2p$/Cu $3d$ cross section from 20 to 25 eV photon energy [25]. The atomic cross sections can explain the strong decrease of the spectral intensities of peaks B and C (which both have significant Cl $3p$ character) and the decrease of the intensity of feature F (which has non-negligible contributions from Cl $3p$ orbitals) on going from 20 to 24 eV photon energy. The fact that there is not a lot of change in the intensity of feature E also follows the trend set by the atomic photoionization cross sections as it is predominantly derived from O $2p$ orbitals. It is, on the other hand, not possible to understand the significant decrease of the spectral intensity of feature A (derived from O $2p$ orbitals) and the vanishing of feature D (predominantly derived from Cu $3d$ orbitals) from 20 to 24 eV photon energy in terms of the O $2p$ and the Cu $3d$ atomic photoionization cross sections.

It was shown that for photon energies varying from 20 to 24 eV, at least some trends in the development of the spectral intensities of the main VB features in the normal emission spectra can be rationalized using atomic Cl $3p$, O $2p$ and Cu $3d$ photoionization cross sections. This is no longer the case in the photon energy range from 50 to

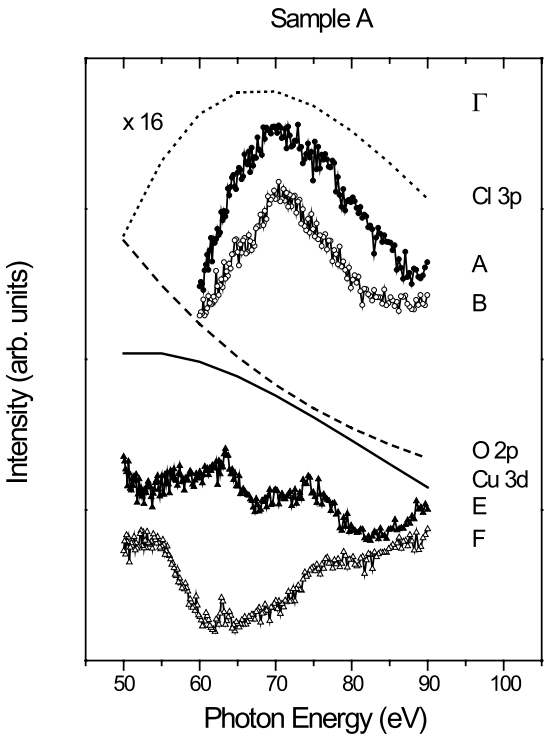

Fig. 5. $Sr_2CuO_2Cl_2$ CIS spectra (lines with symbols) of states in the main VB recorded at normal emission. The states under consideration are denoted using the same notation as in Figure 3. Calculated atomic Cu 3*d* (solid line), O 2*p* (dashed line) and Cl 3*p* (dotted line) photoionization cross sections [25] are shown for comparison. Note that both the CIS spectra and the photoionization cross sections are vertically offset and that the Cl 3*p* cross section is on a different *y*-scale.

90 eV. Figure 5 presents CIS spectra recorded at normal emission for initial-state binding energies corresponding to features A, B, E and F in Figure 4 from 50 to 90 eV photon energy. Also shown are the calculated atomic Cl 3*p*, O 2*p* and Cu 3*d* photoionization cross sections from reference [25]. It is evident that the CIS spectra cannot be reproduced by a linear combination of the atomic photoionization cross sections. It may look like the CIS spectra recorded for initial states corresponding to features A and B follow the Cl 3*p* cross section. But note that the Cl 3*p* cross section is an order of magnitude smaller than the O 2*p* and Cu 3*d* cross sections in this range of photon energies. Only if features A and B were nearly purely derived from Cl 3*p* orbitals, which is evidently not true for feature A and especially not for feature B, would it be expected that CIS spectra A and B would resemble the Cl 3*p* photoionization cross section. The CIS spectra of features E and F bear no resemblance to the atomic cross sections but show spectral structures which are not present in the latter.

It is not possible to explain this spectral structures with a Cu 3*p* to Cu 3*d* resonance as for VB states of a cuprate the Cu 3*p* to Cu 3*d* resonance leads to a dip in the CIS intensity located at ∼74 eV photon energy [26,27]. No such dip at 74 eV photon energy is observed in Figure 5. Furthermore, we have to note that only initial state F has appreciable Cu 3*d* character and that the deviations from the atomic photoionization cross sections are not limited to the vicinity of 74 eV. One could argue that we are not looking at one and the same state for normal emission and fixed binding energy while varying the photon energy since the **k**-component perpendicular to the cleavage plane increases with photon energy (kinetic energy of the photoelectron). If the initial state under consideration has dispersion along the Γ-(0,0,π) direction in **k**-space some change of the character of the state with the momentum component perpendicular to the CuO_2 planes is possible. It is then not expected that the photon energy dependence of the spectral intensity of a feature will be just a linear combination of the atomic photoionization cross sections of the corresponding orbitals with constant coefficients. But as aforementioned, the maximum dispersion of a feature in the normal emission VB spectra of $Sr_2CuO_2Cl_2$ was only ∼0.2 eV in the photon energy range from 20 to 80 eV. Moreover, it is not only for features which are hybridized with chlorine orbitals (*e.g.* features B and F), and for which a dispersion along Γ-(0,0,π) is expected, that the development of the spectral intensity as a function of photon energy is not compatible with the atomic photoionization cross sections of the corresponding orbitals. Features A, D and E, which are purely derived from in-Cu-O-plane orbitals, show the same effect.

Photoelectron diffraction can lead to photoemission intensity variations as a function of photon energy. Firstly, we have to stress that in angle-resolved mode (±1°) and normal-emission geometry only forward- or backward-scattering can scatter photoelectrons into the detector. Assuming that the cleavage plane is in the Sr_2Cl_2 blocks and keeping the small penetration depth of electrons in mind we can limit the discussion to the top Sr_2Cl_2 and CuO_2 layers. There is no atom directly on top of an oxygen atom. There is therefore no chance that photoelectrons originating from an oxygen orbital are scattered into the detector. Consequently, photoelectron diffraction should have no influence on the CIS spectra for initial states A and E which are purely oxygen-derived. Chlorine atoms are on top of copper atoms. Photoelectrons from copper orbitals can then be forward-scattered into the detector which may explain the spectral structures in the CIS spectra of initial state F (predominantly Cu 3*d*-derived). Scattered photoelectrons from chlorine orbitals, on the other hand, can reach the detector only *via* backward-scattering at copper atoms which has a small amplitude. It is therefore doubtful that the deviations of the CIS spectral intensity of initial state B (partly derived from chlorine orbitals) from the corresponding atomic photoionization cross sections is due to photoelectron diffraction.

It is therefore reasonable to conclude that it is predominantly final state effects of the electron-photon matrix element $\langle i|\mathbf{p}\cdot\mathbf{A}|f\rangle$ ($\langle i|$: initial state, **p** photoelectron momentum, **A**: vector potential, $|f\rangle$: final state) which is responsible for the spectral intensities of the VB features of the normal emission spectra of $Sr_2CuO_2Cl_2$ deviating

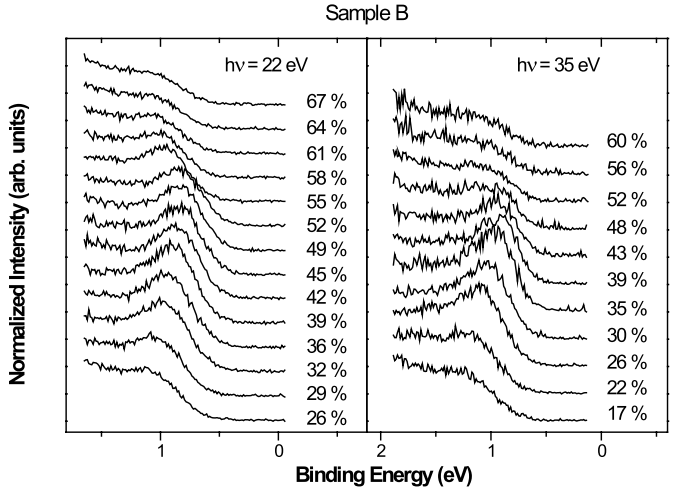

Fig. 6. First electron-removal states of $Sr_2CuO_2Cl_2$ for **k**-vectors from Γ to (π,π) recorded using 22 (left panel) and 35 eV (right panel) photon energy. The **k**-vectors are given in % of the distance between Γ and (π,π).

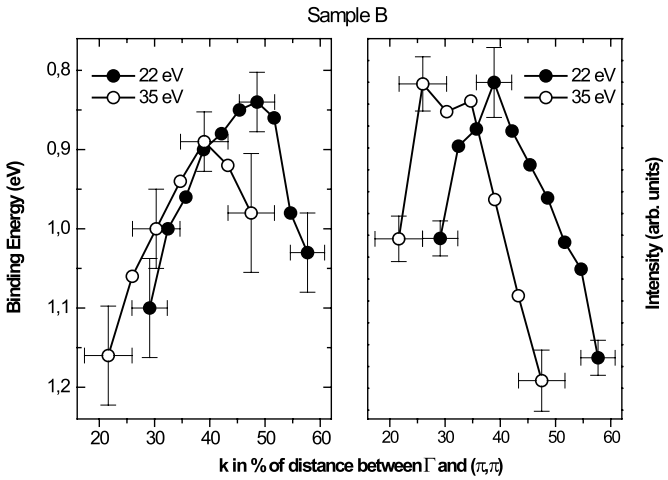

Fig. 7. Binding energy (left panel) and intensity of the peak maxima (right panel) of the first electron-removal states of $Sr_2CuO_2Cl_2$ for **k**-vectors from Γ to (π,π) deduced from the spectra recorded at 22 (solid circles) and 35 eV (open circles) photon energy.

from the trends set by the atomic photoionization cross sections. The final states are not a structureless continuum even for energies 80 eV above the chemical potential.

4.2 Relative intensity and lineshape of the first electron-removal states of $Sr_2CuO_2Cl_2$ as a function of k

In the preceding section it was shown that for $Sr_2CuO_2Cl_2$ the electron-photon matrix element can have a significant influence on the photon energy dependence of the ARPES spectral intensity of a VB feature for photon energies which are typical for ARPES experiments on layered cuprates. In the following, using the first electron-removal states of $Sr_2CuO_2Cl_2$ as an example, we want to demonstrate that for a layered cuprate the electron-photon matrix element can also have a strong impact on the **k**-dependence of the spectral intensity of an ARPES feature as well as on its lineshape which also has an influence on the dispersion relation deduced from the spectra.

Figure 6 presents the first electron-removal states of $Sr_2CuO_2Cl_2$ for **k**-vectors along the Γ to (π,π) direction in **k**-space recorded using 22 and 35 eV photon energy (sample B, sample surface normal in horizontal plane). A distinct low energy peak is observed for each photon energy and the **k**-dependence of the binding energy and the intensity of the peak maximum are displayed in Figure 7. It is evident from Figures 6 and 7 that there are remarkable differences in both the dependence of the spectral intensity on **k** and the dispersion of the low energy peak between the different series of ARPES spectra. As mentioned earlier, for 22 eV photon energy the low energy peak maximum has its lowest binding energy ($\sim$0.84 eV) at $\sim$(π/2,π/2) and the majority of its spectral intensity for **k**-vectors before (π/2,π/2). The maximum of the spectral intensity is at $\sim$40% of the distance between Γ and (π,π). For 35 eV photon energy we observe both differences in the relative strength of the peak and its shape with the latter leading to a dispersion which is different when compared to that deduced from the 22 eV data. For 35 eV photon energy, for example, there is no well developed peak at (π/2,π/2) but only for **k**-vectors between (0.26π,0.26π) and (0.43π,0.43π) while for 22 eV photon energy a distinct peak is observed from (0.29π,0.29π) up to (0.58π,0.58π). The maximum of the spectral intensity is at a smaller **k**-value than for 22 eV photon energy (at $\sim$30% of the distance between Γ and (π,π)) and the dispersion of the low energy peak deduced from the 35 eV ARPES spectra has its minimum binding energy ($\sim$0.89 eV) at $\sim$(0.39π,0.39π) and not at (π/2,π/2). Note that from theory it is expected that the ZRS has its minimum binding energy along Γ to (π,π) at (π/2,π/2) [14]. If one assumes that the ARPES spectral intensity is a perfect image of the spectral function, these results are surprising since the ARPES spectra presented are equivalent in the sense that they show the lowest lying excitations associated with the motion of a hole in an antiferromagnetically ordered CuO_2 plane for **k**-vectors along the Γ to (π,π) direction in the first BZ, *i.e.* the underlying spectral function is the same. In the following we will discuss possible reasons for the observed differences.

We can exclude sample variability as a reason for the observed differences as the spectra presented in Figure 6 were recorded using the same sample and sample cleave in one experimental run. The lack of a well-developed peak in the 35 eV first electron-removal states after (0.43π,0.43π) can not be due to aging of the sample as the spectra were recorded in the order (0.60π,0.60π) first – (0.17π,0.17π) last. As mentioned earlier, our data are in qualitative agreement with all previously published $Sr_2CuO_2Cl_2$ ARPES results recorded for 22.4 [13] and

25 eV photon energy [15]. This also excludes, besides our experimental precautions, the possibility of a misalignment of the samples. Charging can shift spectral intensity to higher binding energy and severly distort spectra, so one could argue that the fact that in the 35 eV ARPES spectra the peak maximum shifts back to higher binding energy before $(\pi/2,\pi/2)$ and also the lack of a distinct peak at **k**-vectors where one such is observed in the 22 eV data is caused by charging. But note that the maximum photon flux during recording of the 35 eV ARPES spectra was still 6 times lower than the minimum photon flux during recording of the 22 eV data, so we would then expect to observe such effects in the 22 eV ARPES spectra too, which is not the case.

From the foregoing discussion we can conclude that the spectra truly represent the low binding energy ARPES response of $Sr_2CuO_2Cl_2$ from Γ to (π,π) at 22 and 35 eV photon energy. As the underlying spectral function is the same in all cases, we cannot explain our ARPES data without involving the electron-photon matrix elements. And indeed, the series of EDC's presented differ in the photoelectron momentum vector **p** and the final state $|f\rangle$ and maybe also the initial state $\langle i|$ (see next paragraph) of the photoexcitation process, factors which affect the electron-photon matrix element. It could be possible that dependent on, for example, photon energy, we would see different initial states but with the shape of the corresponding features in the ARPES spectra and their relative intensities as a function of **k** being representative of the spectral function. In this case we can explain the differences between the 22 and the 35 eV Γ to (π,π) spectra, for example, with the peaks observed in the first electron-removal states of $Sr_2CuO_2Cl_2$ for 22 and 35 eV photon energy each having a different physical origin. But as mentioned earlier, up to now most authors ascribe the peak evident in the first electron-removal states of $Sr_2CuO_2Cl_2$ or $Ca_2CuO_2Cl_2$ to one excitation, the ZRS. It was suggested that a hole in an antiferromagnetically ordered Cu-O plane can decay into spinons and holons as it is the case in one dimension [28]. But the spectral function predicted by the "two-dimensional spinon-holon model" does not show two different peak-like structures but only one peak due to an attractive spinon-holon interaction for **k**-vectors from Γ to (π,π) and a step-like feature for **k**-vectors from Γ to $(\pi,0)$ in contradiction to the experimentally observed broad peak (see right panel of Fig. 1). We have to conclude that according to current knowledge, the first electron-removal states of $Sr_2CuO_2Cl_2$ have to be assigned to a ZRS, *i.e.* one initial state.

It should be evident now that there is no way to understand the differences between the 22 and 35 eV Γ to (π,π) ARPES spectra of $Sr_2CuO_2Cl_2$ without at least assuming that the relative intensity of the ZRS peak in the spectra is strongly affected by the electron-photon matrix element. This is also in agreement with the previously mentioned theoretical results of reference [11] for the ARPES intensities of BSCCO. It still remains to be clarified why the shape of the EDC's of the first electron-removal states of $Sr_2CuO_2Cl_2$ is different for a given **k**-vector using 22 or

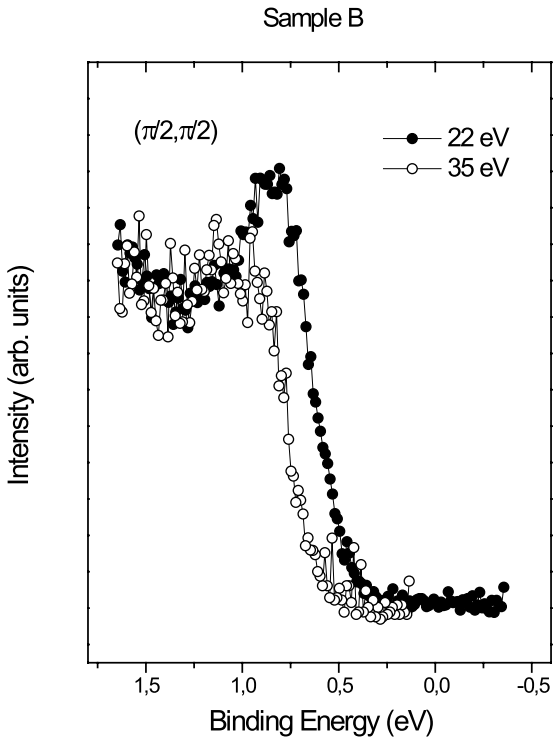

Fig. 8. First electron-removal states of $Sr_2CuO_2Cl_2$ at **k** $\sim(\pi/2,\pi/2)$ recorded using 22 (solid circles) and 35 eV (open circles) photon energy. The spectra are on a different intensity scale for comparison.

35 eV photon energy, which also leads to differences in the dispersion relations deduced from the spectra (Fig. 7).

Let us first summarize some possible reasons for this effect which would not be related to the electron-photon matrix element. Firstly, it could be argued that the peak dispersion could be dependent on the momentum component perpendicular to the cleavage plane. But it should be emphasized that for a ZRS it is not expected that its dispersion is dependent on the momentum component perpendicular to the CuO_2 planes (parallel to cleavage plane) [14]. Another reason could be the background as the ZRS peak sits on a step-like feature which is also observed in the ARPES spectra of the high-temperature superconductors and whose origin is currently unknown. This step-like feature could influence the shape and the position of maximum intensity of the peak ascribed to the ZRS. But judging from spectra where there is no ZRS peak present there seems not to be a lot of change of the shape of this background on going from Γ to (π,π) for the 22 and 35 eV data. The **k**-dependent change of the location of the maximum of the ZRS peak should therefore not been influenced significantly by the background.

On the other hand, there is an explanation of the differences in lineshape and dispersion of the $Sr_2CuO_2Cl_2$ 22 and 35 eV ARPES spectra along Γ to (π,π) if one accepts that the electron-photon matrix element can influence the shape of an individual EDC. In Figure 8 the first electron-removal states of $Sr_2CuO_2Cl_2$ are plotted for a **k**-vector

at $\sim(\pi/2,\pi/2)$ for 22 and 35 eV photon energy (the spectra are scaled in intensity for comparison). Note that the spectra line up very well for binding energies higher than 1 eV. Comparison of the 22 eV and 35 eV spectra reveals that for 35 eV photon energy the ZRS peak seems to be cut. Due to this cut the ZRS peak not only loses intensity but the maximum of the spectral intensity is also shifted to higher binding energy, leading to an apparent dispersion which is different from that deduced from the 22 eV spectra. Although an influence of the electron-photon matrix element on the shape of an ARPES spectrum was not reported for the calculated BSSCO ARPES response of reference [11] we suggest that it is the electron-photon matrix element which is responsible for the photon energy dependent change in the lineshape of the Γ to (π,π) first electron-removal states of $Sr_2CuO_2Cl_2$. A possible reason for this discrepancy between the calculated ARPES response of reference [11] and our findings could be the finite **k**-resolution of our ARPES experiment which in conjunction with possibly significantly different dispersion relations of the final states reached using 22 and 35 eV photons could lead to a different shape of the 22 and 35 eV spectra for the same **k**-vector. Another reason could be that the calculations were performed in the framework of the local-density approximation which is generally not well suited to describe either the lowest lying occupied band of a layered cuprate or the final states 15 eV and more above the Fermi level.

5 Conclusion

In conclusion we have observed that the electron-photon matrix element can have a profound impact on ARPES spectra of the paradigm layered cuprate $Sr_2CuO_2Cl_2$ by significantly affecting the strength *and* the shape of spectral features which can lead to conflicting results regarding the character and the momentum-dependence of energy and spectral weight of a state. This effect has especially to be considered when one has to rely on ARPES spectral intensities as in the case of an analysis of the momentum distribution function n(**k**) [9,17] (the momentum-integrated spectral intensity) and in the angle-scanning mode of angle-resolved photoelectron spectroscopy [29]. Note that in the latter case the changing emission plane-polarization plane geometry may lead to further matrix element related complications which were not addressed in this paper. The results of this study clearly show that in order to get reliable, consistent and complete information about the spectral function of a layered cuprate from an ARPES experiment, the whole parameter range of the ARPES technique should be applied for which purpose synchrotron radiation is ideally suited.

The Ames Laboratory is operated by Iowa State University for the US DOE under Contract No. W-7405-ENG-82. This work is based upon research conducted at the Synchrotron Radiation Center, University of Wisconsin, Madison, which is supported under Award No. DMR-95-31009. M. S. gratefully acknowledges financial support by the II/Aufe program of the German academic exchange service (DAAD).

References

1. C.G. Olson, R. Liu, D.W. Lynch, R.S. List, A.J. Arko, B.W. Veal, Y.C. Chang, P.Z. Jiang, A.P. Paulikas, Phys. Rev. B **42**, 381 (1990).
2. J.C. Campuzano, G. Jennings, M. Faiz, L. Beaulaigue, B.W. Veal, J.Z. Liu, A.P. Paulikas, K. Vandervoort, H. Claus, R.S. List, A.J. Arko, R.J. Bartlett, Phys. Rev. Lett. **64**, 2308 (1990).
3. R.O. Anderson, R. Claessen, J.W. Allen, C.G. Olson, C. Janowitz, L.Z. Liu, J.-H. Park, M.B. Maple, Y. Daliachaouch, M.C. de Andrade, R.F. Jardim, E.A. Early, S.-J. Oh, W.P. Ellis, Phys. Rev. Lett. **70**, 3163 (1993).
4. C.G. Olson, R. Liu, A.-B. Yang, D.W. Lynch, A.J. Arko, R.S. List, B.W. Veal, Y.C. Chang, P.Z. Jiang, A.P. Paulikas, Science **245**, 731 (1989).
5. Z.-X. Shen, D.S. Dessau, B.O. Wells, D.M. King, W.E. Spicer, A.J. Arko, D. Marshall, L.W. Lombardo, A. Kapitulnik, P. Dickinson, S. Doniach, J. DiCarlo, A.G. Loeser, C.-H. Park, Phys. Rev. Lett. **70**, 1553 (1993).
6. D.S. Marshall, D.S. Dessau, A.G. Loeser, C.-H. Park, A.Y. Matsuura, J.N. Eckstein, I. Bozovic, P. Fournier, A. Kapitulnik, W.E. Spicer, Z.-X. Shen, Phys. Rev. Lett **76**, 4841 (1996).
7. H. Ding, T. Yokoya, J.C. Campuzano, T. Takahashi, M. Randeria, M.R. Norman, T. Mochiku, K. Kadowaki, J. Giapintzakis, Nature **382**, 51 (1996).
8. A.G. Loeser, Z.-X. Shen, D.S. Dessau, D.S. Marshall, C.-H. Park, P. Fournier, A. Kapitulnik, Science **273**, 325 (1996).
9. M. Randeria, H. Ding, J.-C. Campuzano, A. Bellman, G. Jennings, T. Yokoya, T. Takahashi, H. Katayama-Yoshida, T. Mochiku, K. Kadowaki, Phys. Rev. Lett. **74**, 4951 (1995).
10. S. Hüfner, *Photoelectron Spectroscopy* (Springer Verlag, Berlin, 1995).
11. A. Bansil, M. Lindroos, J. Phys. Chem. Solids **59**, 1879 (1998); A. Bansil, M. Lindroos, Phys. Rev. Lett. **83**, 5154 (1999).
12. M. Greven, R.J. Birgeneau, Y. Endoh, M.A. Kastner, B. Keimer, M. Matsuda, G. Shirane, T.R. Thurston, Phys. Rev. Lett. **72**, 1096 (1994).
13. B.O. Wells, Z.-X. Shen, A. Matsuura, D.M. King, M.A. Kastner, M. Greven, R.J. Birgeneau, Phys. Rev. Lett. **74**, 964 (1995).
14. E. Dagotto, Rev. Mod. Phys. **66**, 763 (1994).
15. S. LaRosa, I. Vobornik, F. Zwick, H. Berger, M. Grioni, G. Margaritondo, R.J. Kelley, M. Onellion, A. Chubukov, Phys. Rev. B **56**, 525 (1997).
16. C. Kim, P.J. White, Z.-X. Shen, T. Tohyama, Y. Shibata, S. Maekawa, B.O. Wells, Y.J. Kim, R.J. Birgeneau, M.A. Kastner, Phys. Rev. Lett. **80**, 4245 (1998).
17. F. Ronning, C. Kim, D.L. Feng, D.S. Marshall, A.G. Loeser, L.L. Miller, J.N. Eckstein, I. Bozovic, Z.-X. Shen, Science **282**, 2067 (1998).
18. M.S. Golden, H.C. Schmelz, M. Knupfer, S. Haffner, G. Krabbes, J. Fink, V.Y. Yushankhai, H. Rosner, R. Hayn, A. Mueller, G. Reichardt, Phys. Rev. Lett. **78**, 4107 (1997).

19. F.C. Zhang, T.M. Rice, Phys. Rev. B **37**, 3759 (1988).
20. Locations in **k**-space are referenced with respect to the first Brillouin zone (BZ) of the CuO_2 plane and are given in units of the inverse lattice constant of the CuO_2 plane.
21. J.J.M. Pothuizen, R. Eder, N.T. Hien, M. Matoba, A.A. Menovsky, G.A. Sawatzky, Phys. Rev. Lett. **78**, 717 (1997).
22. R. Hayn, H. Rosner, V.Yu. Yushankhai, S. Haffner, C. Duerr, M. Knupfer, G. Krabbes, M.S. Golden, J. Fink, H. Eschrig, D.J. Singh, N.T. Hien, A.A. Menovsky, Ch. Jung, G. Reichardt, Phys. Rev. B **60**, 645 (1999).
23. L.L. Miller, X.L. Wang, S.X. Wang, C. Stassis, D.C. Johnston, J. Faber Jr, C.-K. Loong, Phys. Rev. B **41**, 1921 (1990).
24. R.S. List, A.J. Arko, R.J. Bartlett, C.G. Olson, A.-B. Yang, R. Liu, C. Gu, B.W. Veal, Y. Chang, P.Z. Jiang, K. Vandervoort, A.P. Paulikas, J.C. Campuzano, Physica C **159**, 439 (1989); R.S. List, A.J. Arko, R.J. Bartlett, C.G. Olson, A.-B. Yang, R. Liu, C. Gu, B.W. Veal, J.Z. Liu, K. Vandervoort, A.P. Paulikas, J.C. Campuzano, J. Mag. Magn. Mater. **81**, 151 (1989).
25. J.J. Yeh, I. Lindau, At. Data Nucl. Data Tab. **32**, 1 (1985).
26. J.W. Allen, C.G. Olson, M.B. Maple, J.-S. Kang, L.Z. Liu, J.-H. Park, R.O. Anderson, W.P. Ellis, J.T. Markert, Y. Dalichaouch, R. Liu, Phys. Rev. Lett. **64**, 595 (1990).
27. O. Gunnarsson, J.W. Allen, O. Jepsen, T. Fujiwara, O.K. Andersen, C.G. Olson, M.B. Maple, J.-S. Kang, L.Z. Liu, J.-H. Park, R.O. Anderson, W.P. Ellis, R. Liu, J.T. Markert, Y. Dalichaouch, Z.-X. Shen, P.A.P. Lindberg, B.O. Wells, D.S. Dessau, A. Borg, I. Lindau, W.E. Spicer, Phys. Rev. B **41**, 4811 (1990).
28. R.B. Laughlin, J. Phys. Chem. Solids **56**, 1627 (1995); R.B. Laughlin, Phys. Rev. Lett. **79**, 1726 (1997).
29. P. Aebi, J. Osterwalder, P. Schaller, L. Schlappbach, M. Shimoda, T. Mochiku, K. Kadowaki, Phys. Rev. Lett. **72**, 2757 (1994).